TECHNIQUES by K. Xia, A.J. Rosakis, and H. Kanamori

SUPERSHEAR AND SUBRAYLEIGH TO SUPERSHEAR TRANSITION OBSERVED IN LABORATORY EARTHQUAKE EXPERIMENTS

Vertically dipping crustal faults are long pre-existing weak planes that extend tens of kilometers perpendicular to the earth's surface and often host catastrophic earthquake rupture events. The geometry of such faults is often simple enough to apply appropriately modified concepts of dynamic fracture mechanics to the study of the physics underlying their rupture process. Due to the nature of earthquakes however, direct full field and real time observations of the rupture process are prohibited while even strong motion data, which are useful since they are collected on sites close to fault planes, have limitations of spatial and time resolution. As a result, most efforts to date have focused on complicated analytical studies and on extensive numerical modeling of dynamic rupture processes using finite element, finite difference, and boundary element methods. As clearly elucidated by Rice, Lapusta and Ranjith,[1] the nature and stability of the predicted rupture process depend very strongly on the choice of cohesive or frictional laws employed in the modeling and, as a result, experimental validation of the fidelity of such calculations is of primary importance.

Despite continuous laboratory efforts starting from the early 1970's,[2–4] there are still many mysteries regarding earthquake rupture dynamics. One of the pressing questions is how fast real earthquake ruptures can propagate. As shown by Rosakis,[5] shear cracks in coherent, adhesive, engineering interfaces can propagate at a supershear velocity (faster than the shear wave speed C_s of the material) in various bonded bimaterials subjected to impact loading. However, the question remains on the possibility of supershear growth of a frictional, earthquake type, rupture whose nucleation is spontaneous in nature (absence of stress wave loading) and whose propagation takes place on a mostly frictional, incoherent, interface. Whether and how supershear rupture occurs during earthquakes has important implications for seismic hazards because the rupture speed influences the character of near-field ground motions.

RECENT REPORTS OF SUPERSHEAR EARTHQUAKE FAULT RUPTURE

The M_s 8.1 (M_w 7.8) central Kunlunshan earthquake that occurred on 14 November, 2001, was an extraordinary event from the point of view of dynamic rupture mechanics. The rupture occurred over a long, near-vertical, strike-slip fault segment of the active Kunlunshan fault and featured an exceptionally long (400 km) surface rupture zone and large surface slip displacements. Modeling of the rupture speed history[6] suggests rupture speeds that are slower than the Rayleigh wave speed, C_R, for the first 100 km, transitioning to supershear speed for the remaining 300 km of rupture growth. Other events, such as the 1979 Imperial Valley earthquake,[7,8] the 1992 Landers earthquake,[9] and the 1999 Izmit earthquake[6,10] may also have featured supershear speeds. Even with these estimates at hand, the question of whether natural earthquake ruptures can propagate at supershear speeds is still a subject of active debate. In addition, the exact mechanism for transition from subRayleigh (speed earthquake-type rupture starts with) to supershear rupture speed is not clear. One answer to this question was the two dimensional Burridge-Andrews Mechanism (BAM)[11] which is a mechanism introduced to circumvent restrictions imposed by classical fracture mechanics theories. Classical dynamic fracture theories of growing shear cracks predict that dynamic shear fracture cannot propagate in the small interval between C_R and C_S and thus exclude the possibility of a smooth transition from subRayleigh to supershear. According to the two-dimensional BAM, a shear rupture accelerates to a speed very close to C_R soon after its initiation. A peak in shear stress is found to propagate at the shear wave front and is observed to increase its magnitude as the main rupture speed approaches C_R. At that point, the shear stress peak may become strong enough to promote the nucleation of a secondary micro-rupture whose leading edge propagates at C_P, the longitudinal wave speed of the material. Shortly thereafter, the two ruptures join up and the combination propagates at C_P.[11]

EXPERIMENTAL DESIGN

To answer the above stated questions, we conducted experiments that mimic the earthquake rupture processes. Our goal was to examine the physical plausibility and conditions under which supershear ruptures can be generated in a controlled laboratory environment. We studied spontaneously nucleated dynamic rupture events in incoherent, frictional interfaces held together by far-field tectonic loads. Thus we departed from experimental work that addresses the dynamic shear fracture of coherent interfaces loaded by stress waves.[5,12] In this study, a fault is simulated using two photoelastic plates (Homalite) held together by friction and the far-field tectonic loading is simulated by far-field precompression (Fig. 1a–c). The diagnostics are photoelasticity combined with high-speed photography (up to 10^8 frames per second). The fault system is simulated by using two photoelastic plates (Homalite-100, shear modulus G = 1.4 GPa, Poisson's ratio ν = 0.35, density ρ = 1200 kg/m^3) held together by friction with a dimension of 150 mm × 150 mm. The interface (fault) is inclined at an angle α to the horizontal promoting strike-slip rupture events (Fig. 1a). The carefully prepared interface has a measured static coefficient of friction μ^s = 0.6; the dynamic coefficient of friction μ^d is estimated by finding the critical α of triggered events, which is between 10° and 15°, and hence μ^d = 0.2 is estimated.

K. Xia (SEM Member) is a Ph.D. Candidate, A.J. Rosakis (SEM Member) is a Professor, and H. Kanamori is a Professor at the California Institute of Technology, Pasadena, CA.

This paper received the 3rd Place Award at the 2003 SEM Annual Student Paper Competition held in Charlotte, North Carolina, June 2–4, 2003. The annual Student Paper Competition is organized by Dr. John Ligon of Michigan Technological University.

SUPERSHEAR AND SUBRAYLEIGH

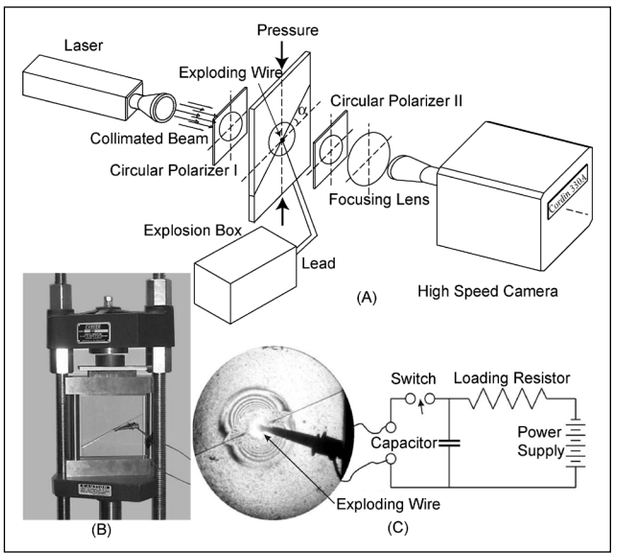

Fig. 1: Experimental setup

The far-field tectonic loading is simulated by uniaxial compression exerted at the top and bottom ends of the system by a hydraulic press (Fig. 1b). The dynamic rupture is nucleated at the center of the simulated fault by producing a local pressure pulse in a small area of the interface. A thin wire of 0.1 mm in diameter is inserted in a small hole of the same size. An electronic condenser is then discharged turning the metal into expanding plasma to provide the controllable pressure pulse (Fig. 1c). The collimated laser beam is extended to a diameter of 100 mm passing through polarizers and transparent specimen before it is focused to the high speed camera. The polarizers are so arranged that isochromatic fringe patterns are obtained. The fault forms an acute angle with the compression axis to provide the shear driving force for continued rupturing.

A unique device that triggers the rupture in a highly controlled manner is used to nucleate the dynamic rupture while preserving the spontaneous nature of the rupturing. This triggering is achieved by an exploding wire technique. The triggering mechanism is inspired by recent numerical work on rupture along frictional interfaces.[11,13,14] Experimentally, it is a convenient way of triggering the system's full-field, high-speed diagnostics (Fig. 1a) that would otherwise be unable to capture an event with total duration of ~50 μs. Before the explosion, the shear traction along the fault is balanced by the static friction force, which is smaller than the maximum static friction force. After the explosion, the local normal traction along the fault is reduced and so is the static frictional force. As a result, the shear traction, which is initially smaller than the static frictional force and unaffected by the isotropic explosion, can be larger than the reduced frictional force momentarily. The resulting net driving force will drive the slip along the interface. Furthermore, the slip will reduce the coefficient of friction as described by either slip-weakening, slip-rate-weakening or the state and rate dependent friction law; in other words, the friction changes from static friction to dynamic friction. If the original shear traction is larger than the dynamic friction, the slip will continue to propagate away from the explosion site (corresponding to the hypocenter of an earthquake) where normal traction reduction due to the explosion is not important any more. This way, a spontaneous rupture or laboratory earthquake is triggered.

EXPERIMENTAL RESULTS

Experiments featuring a range of α and far-field pressure P were performed and the symmetric bilateral rupture process histories were visualized in intervals of 2 μs. Depending on P and α, rupture speeds that are either subRayleigh or supershear were observed.

Figure 2 displays isochromatic (maximum in-plane shear stress field) snapshots of examples of purely subRayleigh wave speed ruptures from two experiments. In Fig. 2a–b the inclination angle is 20° and P = 13 MPa. The speed of the rupture tip (indicated by the arrow) is very close to C_R and follows very closely behind the circular shear wave front, which is emitted at the time of rupture nucleation. In Fig. 2c–d the inclination angle is 25° and P = 7 MPa. The speed of the rupture tip (indicated by the arrow) is again found to be very close to C_R. The same phenomenon was observed for either smaller inclination angles or lower uniaxial pressure P.

In Fig. 3, the inclination angle was kept at 25° while the pressure was increased to 15 MPa. For comparison purposes, the same time instants (28 μs and 38 μs after nucleation) are displayed. In this case, the circular traces of the shear wave are also visible and are at the same corresponding locations as in Fig. 2. However, in front of this circle, supershear disturbances (propagating to the northwest, marked in the photograph as the Rupture-tip and featuring a clearly visible Mach cone) are shown. The formation of the Mach

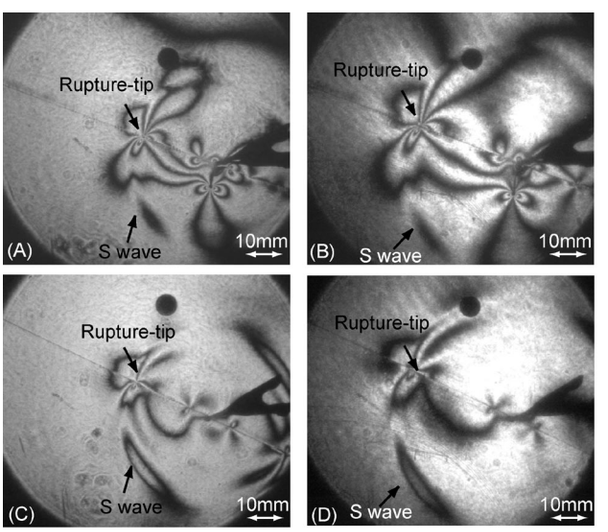

Fig. 2: Earthquake experimental results of purely subRayleigh cases. A and B are from one experiment with a pressure of P = 13 MPa and angle α = 20° at the time instants of 28 μs and 38 μs respectively. C and D are from one experiment with a pressure of P = 7 MPa and angle α = 25° at the time instants of 28 μs and 38 μs respectively.

SUPERSHEAR AND SUBRAYLEIGH

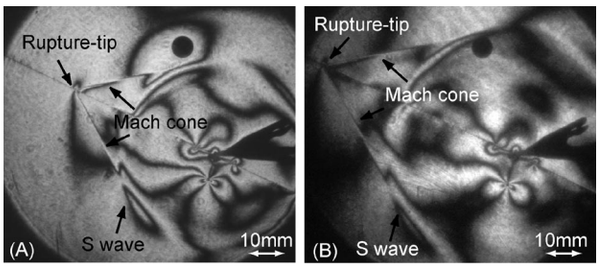

Fig. 3: Earthquake experimental results of purely supershear case. A and B are from one experiment with the pressure of P = 13 MPa and angle α = 25° at the time instants of 28 μs and 38 μs respectively.

cone is due to the fact that the rupture is propagating faster than the shear wave speed of the material. For this case, the sequences of images other than those at 28 μs and 38 μs have a very similar form and reveal a disturbance that was nucleated as supershear. Its speed history $v(t)$ is determined independently by either differentiating the rupture length history record or by measuring the inclination angle, δ, of the shear shocks with respect to the fault plane and using the relation $v = C_S/\sin\delta$. Its speed was 1970 m/s, which is close to the longitudinal wave speed C_P. This is the first experimental report of the supershear of a spontaneous shear rupture to our knowledge. The supershear rupture initiated right after the triggering of the earthquake rupture, which can be seen from the fact that the Mach cones are tangential to the shear wave front.

As discussed earlier, we are interested in investigating how the supershear rupture nucleated experimentally. For the experimental results above, the supershear was nucleated immediately after the triggering. Since the rupture speed is controlled by both the inclination angle α and the magnitude of uniaxial compression P, it is possible for us to vary both of them carefully to delay the appearance of supershear rupture. Specifically, we fix the inclination angle α at 25° and decrease P in order to capture the nucleation process of a supershear rupture.

Figure 4a–d corresponds to a case with an intermediate far-field pressure as compared to the ones displayed in Fig. 2c–d and Fig. 3. Here, the angle is kept the same (25°) and the pressure is decreased to 9 MPa in an attempt to visualize a transition within our field of view (100 mm). Four different time instances of the same rupture event are displayed. In Fig. 4a, the circular trace S waves are visible followed by a rupture propagating at C_R. At the shear wave front, we can see a small angular feature which is corresponding to a shear stress peak and is not visible at the shear wave fronts in Fig. 2. In Fig. 4b, a small secondary rupture appears in front of the main rupture and propagates slightly ahead of the S wave front. In Fig. 4c–d, the two ruptures coalesce and the leading edge of the resulting rupture grows with a speed at a speed of 1970 m/s which is very close to C_P.

Figure 5 displays the length vs. time of the two ruptures. The length scale is a direct reading from pictures corresponding to the test shown in Fig. 4. Before and after their coalescence, we compared their slopes to the characteristic

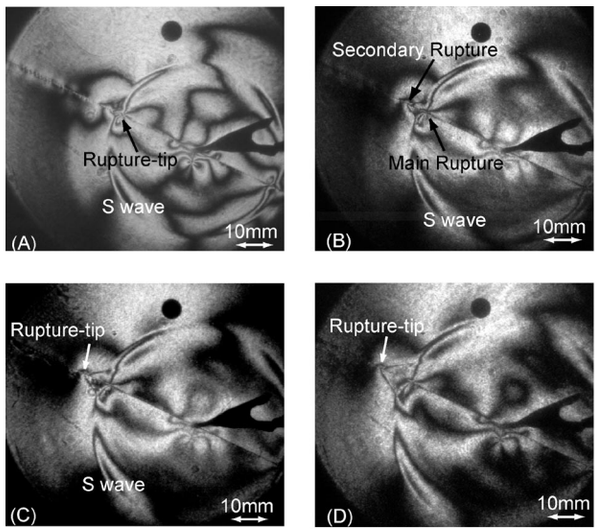

Fig. 4: Visualization of the subRayleigh to supershear rupture transition. A–D are taken at 28 μs, 30 μs, 32 μs and 34 μs respectively.

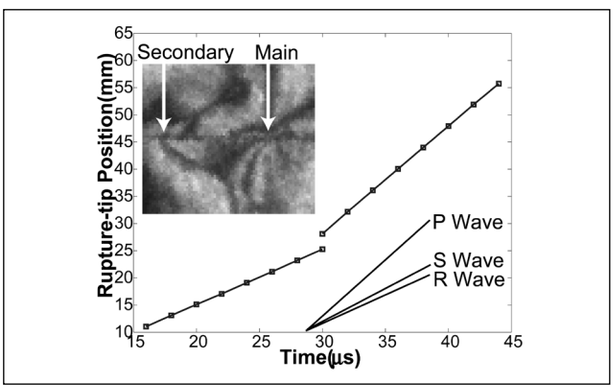

Fig. 5: Rupture-tip history showing subRayleigh to supershear transition

wave speeds of the material. The 3-D P wave speed and S wave speed of the material are measured using 5 MHz ultrasonic transducers. We then calculated the plane stress P wave speed and plot the slopes corresponding to plane stress P, S and Rayleigh wave speeds in the Fig. 5. It also shows a magnified view of the secondary rupture as it nucleates in front of the main rupture and both ruptures are indicated by arrows. For this case, the transition length L, which measures the distance from the triggering location to the initial position of the supershear rupture-tip, is approximately 20 mm.

CONCLUSIONS

In conclusion, we designed an experimental setup to study the dynamics of an earthquake rupturing process. With a unique triggering mechanism, we are able to mimic the earthquake ruptures which are spontaneous in nature. We observed supershear earthquake ruptures and furthermore, the subRayleigh to supershear rupture transition. The tran-

sition mechanism qualitatively conforms to the well-known Burridge-Andrews mechanism.

ACKNOWLEDGEMENTS

The authors appreciate fruitful discussions with Prof. G. Ravichandran from Caltech and Prof. J.R. Rice from Harvard. This study is supported by NSF grant EAR-0207873 and ONR grant N00014-03-1-0435.

References

1. Rice, J.R., Lapusta, N., Ranjith, K. *Rate and state dependent friction and the stability of sliding between elastically deformable solids.* Journal of the Mechanics and Physics of Solids, 2001. **49**(9): p. 1865–1898.

2. Scholz, C., Molnar, P., Johnson, T. *Detailed Studies of Frictional Sliding of Granite and Implications for Earthquake Mechanism.* Journal of Geophysical Research, 1972. **77**(32): p. 6392–&.

3. Wu, F.T., Thomson, K.C., Kuenzler, H. *Stick-Slip Propagation Velocity and Seismic Source Mechanism.* Bulletin of the Seismological Society of America, 1972. **62**(6): p. 1621–1628.

4. Brune, J.N. *Earthquake Modeling by Stick-Slip Along Precut Surfaces in Stressed Form Rubber.* Bulletin of the Seismological Society of America, 1973. **63**(6): p. 2105–2119.

5. Rosakis, A.J., Samudrala, O., Coker, D. *Cracks faster than the shear wave speed.* Science, 1999. **284**(5418): p. 1337–1340.

6. Bouchon, M., Vallee, M. *Observation of long supershear rupture during the magnitude 8.1 Kunlunshan earthquake.* Science, 2003. **301**(5634): p. 824–826.

7. Archuleta, R.J. *A Faulting Model for the 1979 Imperial-Valley Earthquake.* Journal of Geophysical Research, 1984. **89**(NB6): p. 4559–4585.

8. Spudich, P., Cranswick, E. *Direct Observation of Rupture Propagation During the 1979 Imperial Valley Earthquake Using a Short Baseline Accelerometer Array.* Bulletin of the Seismological Society of America, 1984. **74**(6): p. 2083–2114.

9. Olsen, K.B., Madariaga, R., Archuleta, R.J. *Three-dimensional dynamic simulation of the 1992 Landers earthquake.* Science, 1997. **278**(5339): p. 834–838.

10. Bouchon, M., et al. *Space and time evolution of rupture and faulting during the 1999 Izmit (Turkey) earthquake.* Bulletin of the Seismological Society of America, 2002. **92**(1): p. 256–266.

11. Andrews, D.J. *Rupture Velocity of Plane Strain Shear Cracks.* Journal of Geophysical Research, 1976. **81**(32): p. 5679–5687.

12. Rosakis, A.J. *Intersonic shear cracks and fault ruptures.* Advances in Physics, 2002. **51**(4): p. 1189–1257.

13. Cochard, A., Rice, J.R. *Fault rupture between dissimilar materials: Ill-posedness, regularization, and slip-pulse response.* Journal of Geophysical Research-Solid Earth, 2000. **105**(B11): p. 25891–25907.

14. Andrews, D.J., Ben-Zion, Y. *Wrinkle-like slip pulse on a fault between different materials.* Journal of Geophysical Research-Solid Earth, 1997. **102**(B1): p. 553–571. ■